

# A Highly Sensitive Capacitive Touch Sensor Integrated on a Thin-Film-Encapsulated Active-Matrix OLED for Ultrathin Displays

Sunkook Kim, Woong Choi, Woojin Rim, Youngtea Chun, Hongsik Shim, Hyukjun Kwon, Jongsoo Kim, Inseo Kee, Sungchul Kim, SangYoon Lee, and Jongsun Park

**Abstract**—This paper presents ultrathin and highly sensitive input/output devices consisting of a capacitive touch sensor (Cap-TSP) integrated on thin-film-encapsulated active-matrix organic light-emitting diodes (OLEDs). The optimal structure of the electrically noise-free capacitive touch sensor, which is assembled on a thin-film-encapsulated active-matrix OLED (AMOLED) display, is obtained by investigating the internal electrical field distribution and capacitance change based on the Q3D Extractor model. Electrostatic simulations have verified malfunction-free electrical signals for 4-in diagonal-sized capacitive touch sensors on AMOLEDs possessing a 100- $\mu\text{m}$ -thick optically clear adhesive (OCA,  $\epsilon_r = 1.4$ ) layer. The prototype OLED platform using the capacitive touch sensors exhibits an overall thickness of 1.2 mm, which is the lowest thickness for commercially available OLED platforms.

**Index Terms**—Active-matrix organic light-emitting diode (AMOLED), capacitive touch sensor (Cap-TSP), noise, ultrathin display.

## I. INTRODUCTION

THE DEMAND for display technologies that are ultrathin and mechanically flexible has attracted a great deal of attention, as they allow for a small form factor and versatile design and are lightweight and easily portable. Significant progress has been made in achieving a flexible active-matrix organic light-emitting diode (OLED) [1]–[3], a foldable/seamless OLED display [4], [5], and a robust rollable active-matrix OLED (AMOLED) display [6]. The proof of concept for these types of displays [2], [3] was demonstrated by forming a neutral plane under the regime of an OLED/thin-film transistor (TFT) integrated circuit with two supporting plastic layers, where the neutral plane is defined as a strain-free zone under inward and outward bending pressures [7], [8]. OLED/TFTs were manufactured on the bottom supporting plastic layer (a 500- $\mu\text{m}$ -thick

Manuscript received March 22, 2011; revised June 20, 2011 and July 15, 2011. Date of publication August 18, 2011; date of current version September 21, 2011. The review of this paper was arranged by Editor J. Kanicki.

S. Kim, W. Choi, Y. Chun, H. Shim, H. Kwon, and S. Lee are with the Samsung Advanced Institute of Technology, Yongin-si 446-712, Korea (e-mail: sangyoon.lee@samsung.com).

W. Rim, and J. Park are with the School of Electrical Engineering, Korea University, Seoul 136-713, Korea (e-mail: jongsun@korea.ac.kr).

J. Kim, I. Kee, and S. Kim are with the Samsung Mobile Display, Yongin-si 446-712, Korea.

Color versions of one or more of the figures in this paper are available online at <http://ieeexplore.ieee.org>.

Digital Object Identifier 10.1109/TED.2011.2162844

polyimide film); any plastic film with the same thickness can be used as the upper protection layer. We previously reported on the possible application of highly flexible OLED display components based on microcavities, thin-film encapsulation, and low-temperature color filters [4], [5]. Currently, flexible OLED displays preserve the outstanding performance of OLED technology; however, they must solve the challenge of an intuitive user interface between the display and a human user.

Touch sensors have been actively studied for use in an intuitive user interface in mobile displays. Since the discovery of four-wire resistive touch screens in 1997 [9], resistive, capacitive [10]–[12], surface acoustic wave [13], and infrared ray [14] techniques have been recently used for sensing touch inputs on touch-screen devices. Among these techniques, resistive touch screens have been widely used in commercial mobile displays. Resistive touch sensors are composed of two parallel layers of conductive indium tin oxide (ITO) with an insulating interlayer between them, where the event of touching the top layer changes the resistance of the two ITO layers and thereby defines the location of the user's touch. However, the resistive touch method has major drawbacks, such as the weakness of the ITO layers at high pressures and the nonavailability of multitouch algorithms.

In response, capacitive touch panels (Cap-TSP) are becoming incredibly popular due to their high durability, unlimited multitouch functionality, and excellent optical transparency. As shown in Fig. 1, a Cap-TSP is basically built using two conductive electrodes in parallel (two layers) or in series (one layer), where the patterns of the conductive electrodes form a capacitor holding a charge. If the user places another conductive object, such as a finger, near the top surface of the touch screen, the charge field (electrical field) found between the capacitor plates changes because the human body capacitance absorbs the fringing electrical field. The conventional Cap-TSP is manufactured on a glass encapsulation layer (thicker than 500  $\mu\text{m}$ ) in on-cell-type TSPs or with an individual thick isolation layer. In order to integrate highly sensitive Cap-TSPs into an ultrathin-film-encapsulated OLED panel for an ultrathin display, the following requirements are needed: 1) electrical reliability without any sensing malfunction when a touch sensor is directly integrated onto an OLED panel; 2) a low-temperature process in order to prevent deformations in the glass substrate; 3) a high-yield process since, in the case of an on-cell touch screen, the Cap-TSPs are fabricated directly on the OLED panel

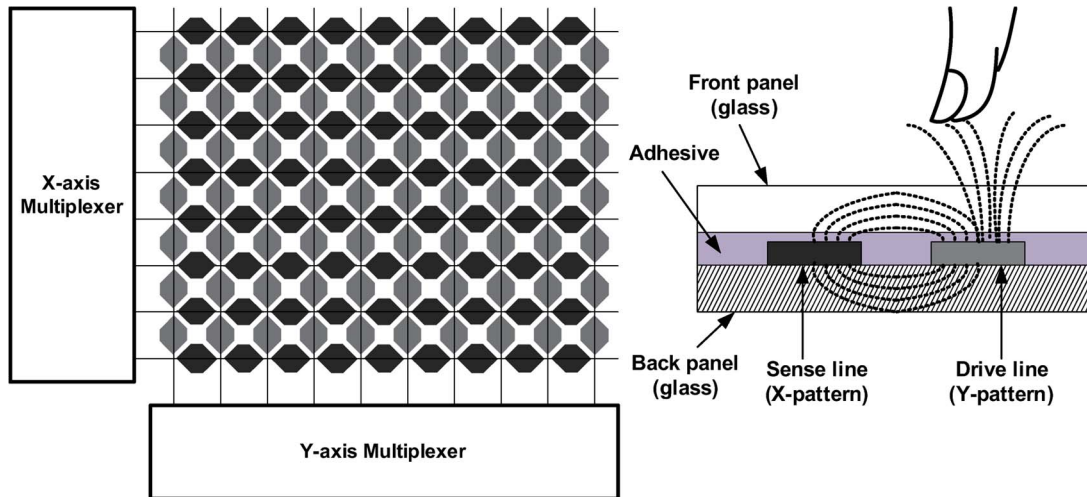


Fig. 1. Capacitive touch sensor panels, with the  $X$ - $Y$  electrodes and their corresponding mutual capacitances in the touch screen.

(therefore, a failure in the TSP process can impact the overall OLED panel yield); and 4) high optical transparency in order to save on power consumption.

In this paper, we report on the first demonstration of a malfunction-free mutual capacitive touch sensor assembled on an ultrathin-film-encapsulated OLED panel that is free of electrical noise. All of the processes used to fabricate the touch sensor have been especially developed to be performed at low temperatures (below 200 °C). The touch sensor is fabricated on a coplanar/single-ITO layer in order to achieve a high optical transmittance of 90%, compared to conventional TSPs composed of two ITO layers. The Cap-TSPs are directly patterned on the protective glass cover, and then, optically clear adhesives (OCAs) bind the two panels (the protective glass cover and the OLED glass panel) without allowing any interaction of the electrical fields through themselves. In order to block the touch electrode fringing fields from reaching the OLED device, an OCA film possessing a low dielectric constant ( $\epsilon_r = 1.4$ ) is used as an interlayer insulator. Furthermore, the theoretical calculations, in contexts ranging from the sensing of the capacitance between the human and touch electrodes to electromagnetic simulations regarding the interference of electrical signal, provides quantitative and predictive understanding of the sensing characteristics for the touch sensor directly integrated on OLEDs. Based on these electrostatic simulations and using advanced fabrication techniques, Cap-TSPs have been realized on a 5.4-in foldable/seamless OLED containing a 100- $\mu\text{m}$ -thick OCA film.

## II. EXPERIMENT DESIGN

### A. Capacitive Touch Sensor Fabrication

Fig. 2(a) shows a schematic view of the capacitive touch sensor fabricated on the protective glass layer (Gorilla glass, CORNING), consisting of an  $18 \times 25$  touch sensor matrix on a 4-in screen. The process starts with the deposition of fully transparent 100-nm-thick ITO using the ion-assisted deposition method. After the snowflake-patterned drive and sense lines are

defined by photolithography, the transparent touch sensor panel possessing a coplanar ITO layer is patterned onto the same side of the cover glass using an ITO wet etchant for 1 min. Fig. 2(a) shows a representative capacitive touch sensor with which the coplanar ITO layer forms the drive (columnlike metal trace as  $Y$ -axis coordinator) and sense lines (rowlike metal trace as  $X$ -axis coordinator). The  $Y$ -axis coordinators in an individual column-ITO trace are directly connected in the border area; the  $X$ -axis coordinators in the ITO trace row are individually separated. Thus, the ITO patch terraces need to be bridged using a separate  $X$ -axis ITO coordinator. When a finger touches the  $X$ - $Y$  coordinator pixel, the fringing electric field between the adjacent  $X$ -coordinator and  $Y$ -coordinator within the coplanar side is blocked by the finger, reducing the amount of charge coupled on the pixel. However, in the coplanar ITO  $X$ - $Y$  layer structure, a 300-nm-thick low temperature  $\text{SiO}_2$  insulator is deposited at 200 °C under the terrace electrode bridge as an isolating layer to avoid a short between the  $X$ - $Y$  coordinator, as shown in Fig. 2(a). A contact hole in the shape of the terrace is created by using isotropy dry etching utilizing a gas flow of  $\text{CHF}_3$  at 25 sccm,  $\text{O}_2$  at 15 sccm, and Ar at 60 sccm at 75 mtorr for 3 min at room temperature so that a thin ITO layer can bridge the border of the two  $X$ -axis coordinators. Finally, the touch panel is passivated using a 200-nm-thick low-temperature  $\text{SiO}_2$  layer. Fig. 2(b) shows the layout design of the snowflake  $X$ - $Y$  coordinates of the capacitive touch sensor. Fig. 2(c) shows the measured optical transmission spectra in the visible range for the finished CTS. The measured optical transmission in the 300–800-nm wavelength range is on the average of 91%. Typically, conventional touch sensors composed of two ITO layers have their transparency limited to less than 80%; however, the co-planner  $X$ - $Y$  coordinator fabricated on a single side of a substrate affords transparencies as high as 90%. This system also has low power consumption, which decreases the required luminance and reduces the parasitic capacitance. Furthermore, the thin-coplanar CTS has several advantages, in that it can easily be bent or rolled to provide superb mechanical stability and can be considerably slimmer and lighter than current platforms.

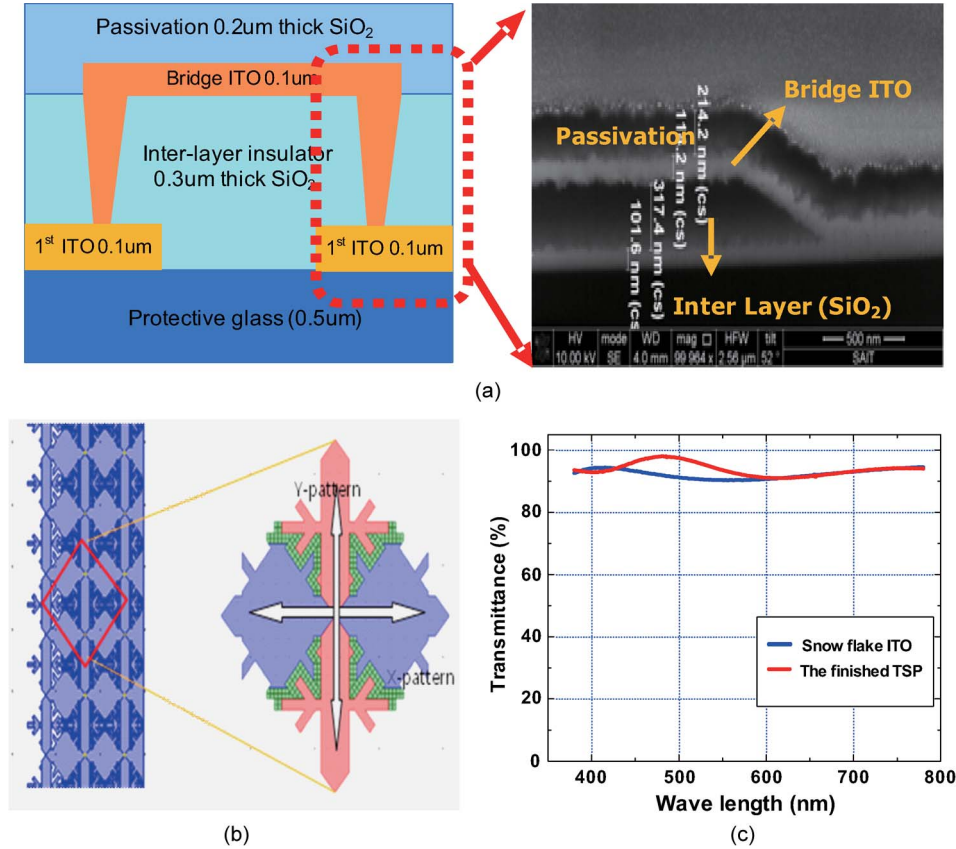


Fig. 2. (a) Schematic view of a capacitive touch sensor. (Inset) SEM image of the bridge pattern at the cross of the  $X$ - $Y$  coordinator. A 300-nm-thick low-temperature (LT)  $\text{SiO}_2$  insulator helps to isolate the  $X$ - $Y$  coordinators to prevent electrical shorts. (b) Top view of the layout of an exemplary column ( $Y$ ) and adjacent row patches ( $X$ ) for the snowflake-patterned capacitive touch sensor coplanar ITO layer. (c) Optical transmission spectra as a function of wavelength through the Cap-TSP.

**B. Capacitive Touch Sensing Operation**

The main capacitive touch sensing principle is to detect the change in capacitance when a user touches the screen. As shown in Fig. 1, the  $X$ - $Y$  grid in the touch screen is made by etching a layer to form a pattern of electrodes. As can be seen, mutual capacitances are observed at the intersections of two electrodes, which are due to the fact that the two conductive objects (the  $X$ - $Y$  electrodes) are able to hold a charge if they are very close together. A human finger placed near the intersection of two electrodes changes the mutual capacitance value; sensing circuitry measures these capacitance changes. The changes of the capacitance are mainly due to the fact that a finger disturbs the fringing electric field above the sensor, which means that some of the charge is transferred to the user and so reduces the capacitance between the electrodes. In order to detect the capacitance variation, several techniques such as successive approximation [15], a relation oscillator [16], [17], and an  $RC$  delay technique [18] have been studied. One of the most effective techniques is found in the charge transfer approach, where a higher sensing sensitivity can be achieved since only the amount of transferred charge is sensed [19].

A capacitive touch sensing operation using the charge transfer approach is shown in Fig. 3. A switched capacitor circuit is used to assess the relative change in a sensor’s capacitance when the screen is being touched.  $C_{XY}$  is the unknown mutual capacitance found between two electrodes ( $X$ - $Y$  patterns), and

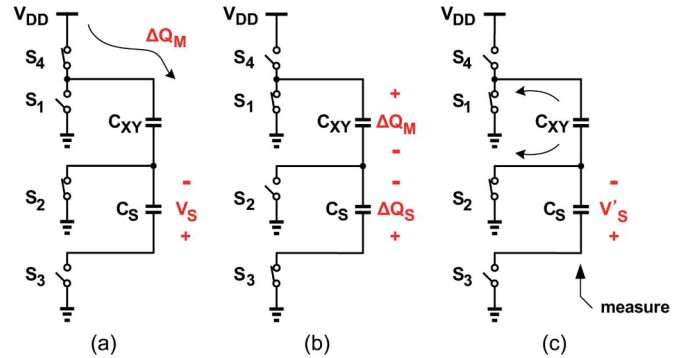


Fig. 3. Charge transfer operation. (a) Charge state. (b) Transfer state. (c) Measurement state.

$C_S$  is the sampling capacitor embedded in the touch sensor that possesses a much larger capacity than  $C_{XY}$ . (Typically,  $C_S$  is 100 times larger than  $C_{XY}$ .) Initially, switches  $S_1$  and  $S_2$  are closed in order to discharge  $C_{XY}$ . The sensing operation involves the following three stages: First, switches  $S_2$  and  $S_4$  are closed in order to charge  $C_{XY}$ . Second,  $S_2$  is opened, and  $S_1$  and  $S_3$  are closed, sharing the stored charge on  $C_{XY}$  with  $C_S$ . Finally,  $S_2$  closes, and  $S_3$  is opened in order to measure the voltage across  $C_C$ . The resulting voltage across  $C_S$  is proportional to the charge transferred from  $C_{XY}$  to  $C_S$ .

In the “charge” state shown in Fig. 3(a),  $\Delta Q_M$  represents the charge transfer from the  $V_{DD}$  supply voltage to  $C_{XY}$ .  $V_S$  is the

voltage across  $C_S$ , which can be expressed as  $V_S = \Delta Q_S / C_S$ .  $\Delta Q_S$  is defined by the stored charge on  $C_S$ . During the transfer stage [Fig. 3(b)],  $\Delta Q_M$  and  $\Delta Q_S$  are shared by  $(C_{XY} + C_S)$ . Therefore, the voltage across  $C_S$  at the measurement stage [Fig. 3(c)] is

$$V'_S = \frac{\Delta Q_S - \Delta Q_M}{C_S + C_{XY}} = \frac{C_S}{C_S + C_{XY}} V_S - \frac{C_{XY}}{C_S + C_{XY}} V_{DD}. \tag{1}$$

Since  $C_S$  is much larger than  $C_{XY}$  ( $C_S \gg C_{XY}$ ), (1) can be approximated as

$$V'_S \approx V_S - \frac{C_{XY}}{C_S} V_{DD}. \tag{2}$$

In (2), the  $V_S$  term is the result from the charge transferred during the previous cycle; the  $(C_{XY}/C_S)V_{DD}$  term is defined by the decreasing voltage due to the transferred charges. It should be noted that the decreasing voltage is directly proportional to the mutual capacitance ( $C_{XY}$ ).

By repeating these operation cycles, the voltage across  $C_S$  decreases toward the ground voltage. Since the decreasing voltage rate is proportional to  $C_{XY}$ , the relative value of  $C_{XY}$  can be determined by counting the number of cycles that are needed for the voltage ( $V'_S$ ) to go down to a given threshold voltage. When a user touches the screen, the finger steals a charge from  $C_{XY}$ . In other words, the touch input makes the mutual capacitance  $C_{XY}$  between the electrodes smaller, which results in taking more cycles for  $C_S$  to discharge to the threshold voltage.

Fig. 4 shows the touch sensing circuitry using the charge transfer approach. It consists of ramp-up resistor ( $R_1$ ), comparator, capture register, and counter. When the counter starts,  $S_5$  is opened, and  $S_6$  is closed in order to set the initial voltage of  $C_S$  to the supply voltage  $V_{DD}$ . During the sensing operation, the voltage on  $C_S$  decreases, and when the voltage crosses the threshold voltage ( $V_T$ ), the capture register latches the counter's output. When a human finger is not placed on the screen, the charge on  $C_S$  is transferred relatively quickly, thus generating a small counter value. Conversely, when a finger is placed on the screen, since the charge is transferred more slowly, the latched counter value is larger. The timing diagram of the sensing operation is illustrated in Fig. 4.

### III. RESULTS AND DISCUSSIONS

#### A. Physical Structure of the AMOLED Display

Fig. 5 shows a schematic view of the capacitive touch sensors integrated onto the thin-film-encapsulated OLED display. The implementation of the OLED panel starts with low-temperature poly-Si TFTs used to switch/drive the OLED devices; top-emission Red/Green/Blue (RGB) OLED devices are then formed on the TFT circuits. The top-emission RGB pixels comprise the following: 1) a bilayer Ag (200 nm)/ITO (10 nm) anode; 2) an OLED device incorporating a multi-layer hole-injection-layer/hole-transport-layer/emissive-layer/electron-transport-layer OLED layer; 3) a bilayer of Mg:Ag (10:1, 15 nm) cathode; and 4) an organic capping layer. The upper layer of the top-emission OLED display is specially

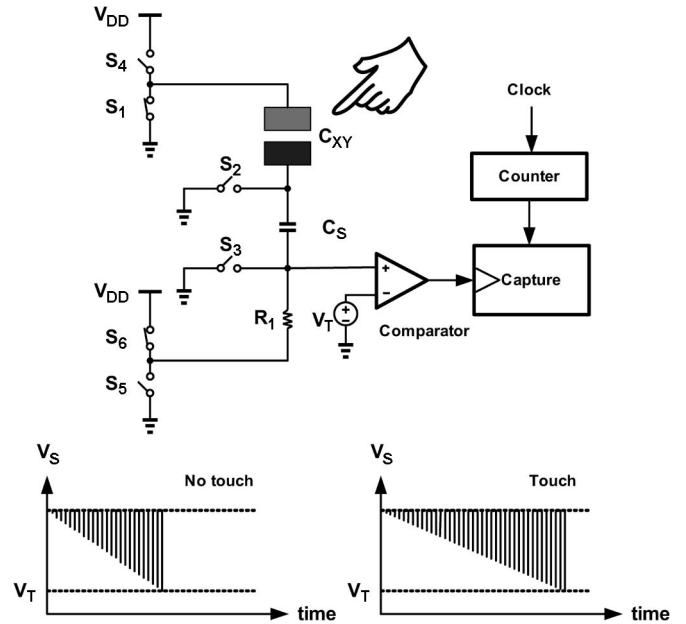


Fig. 4. Capacitive touch sensor circuitry and the timing diagram of the sensing operation.

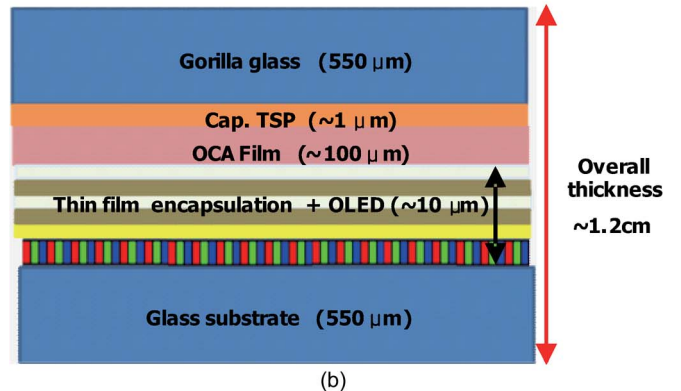
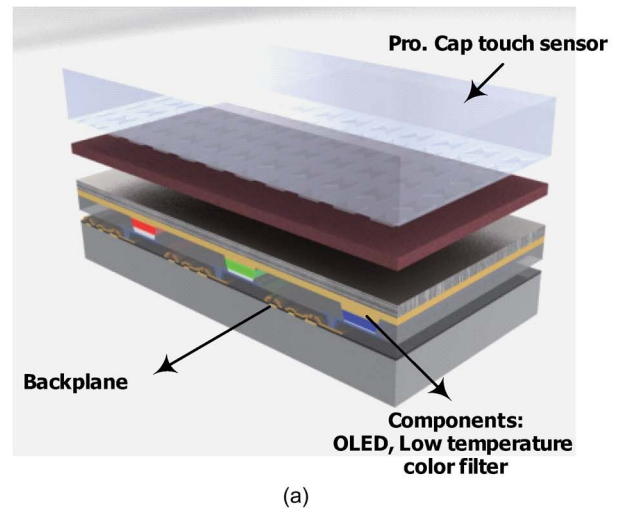


Fig. 5. (a) Cross-sectional diagram of the ultrathin AMOLED display using Cap-TSPs composed of thin-film encapsulation and RGB OLED microcavities. The Cap-TSP is fabricated on the underside of the glass protection layer. (b) Overall thickness of the OLED panel with the TSP is 1.2 mm, which is considerably slimmer and lighter than current display platforms. (Currently, the thinnest commercially available display platform is reported to be 8.9 mm.)

designed to form a coplanar single-layer cathode electrode, thus acting as an electrical ground used to generate the same electrostatic potential. In order to defend the OLEDs from oxygen and water, they are encapsulated with a multilayered thin film composed of an oxide layer (200–500-nm-thick  $\text{Al}_2\text{O}_3$ ) as a barrier and polymer layer (0.25–1  $\mu\text{m}$ ) as a planarization layer using Barix<sup>TM</sup> (produced by Vitex). The total thickness of the multilayered thin-film encapsulation is of only several micrometers, which is considerably thinner than the conventional glass encapsulation method. (Currently, commercial glass encapsulations have a thickness of 500  $\mu\text{m}$ , which is two orders of magnitude higher than that of the proposed thin-film-encapsulation method.) Although thin-film encapsulation allows OLED displays to be thinner and protects the OLEDs from oxygen and water, the thin interlayer typically can cause difficulties in shielding the electrical signal of the TSP from the OLED panel since the fringing field from the TSP electrodes can be easily transmitted to the OLED pixel cathode layer. (Note that the TSPs on the cover glass are isolated from the OLED panel.) The final process used to integrate the two panels is by simply laminating the Cap-TSP onto the OLED panel using heat and pressure. Commercially available 3M OCA is utilized not only as an adhesive but also as an electrical insulator in order to protect against fringing field losses from the Cap-TSPs to the OLED pixel cathode electrodes.

### B. Analysis of Electromagnetic Simulation and Parasitic Extraction for the Capacitive Touch Screen on the OLED Display

Fig. 6 shows the contours of the electric field obtained from the simulation (Q3D Extractor, Ansoft) along with a model. As previously mentioned, the OCA film isolates the electrical signal leakage between the TSPs and OLEDs, which is a material with a low dielectric constant ( $\epsilon_r = 1.4$ ). The empirical model is performed in order to obtain the physical structure parameters, as shown in the inset of Fig. 6(a). For the simulation, the  $C_{XY}$  between the  $X$ – $Y$  electrodes is monitored as a function of the thickness of the OCA films, where the dielectric constant of the OCA layer and the dielectric constant of the thin-film-encapsulation layer are assumed to be 1.5 and 7, respectively. Without a finger, as can be seen in Fig. 6(b), the fields are mostly contained between the  $X$  and  $Y$  patterns, generating capacitance  $C_{XY}$  between them. As a user touches the panel with a finger, Fig. 6(c) shows that the electric fields are diverted from  $C_{XY}$  to ground through the finger, reducing the  $C_{XY}$  value. Because a reduced OCA thickness results in thinner display devices, it is important to estimate the minimum OCA thickness needed to maintain the sensitivity of the  $C_{XY}$  difference between the two cases with respect to electrical noise. Fig. 6(d) shows  $C_{XY}$  with and without a finger, respectively, versus the OCA thickness. For the given OCA thickness range, the  $C_{XY}$  has a range of 0.33–0.86 pF (without a finger) and 0.17–0.55 pF (with a finger). While the  $C_{XY}$  variation maintains a consistent 0.4 pF at a thickness between 80 and 300  $\mu\text{m}$ , it shows noticeable reduction at a thickness below 80  $\mu\text{m}$ . Therefore, the sensitivity will be good as long as the OCA film is equal to or thicker than 80  $\mu\text{m}$ .

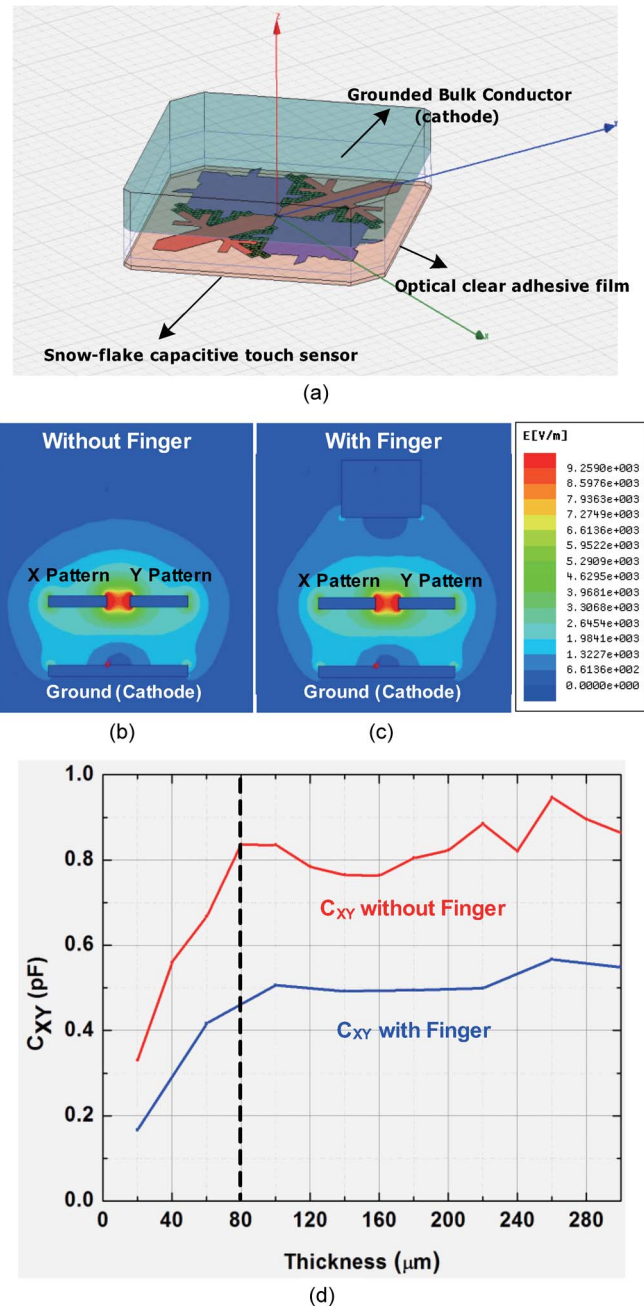


Fig. 6. (a) Q3D Extractor projector illustrating the physical dimensions of the overall schematic view of the OLED and Cap-TSP shown in Fig. 4. The distribution of the electrostatic field (b) without a finger or (c) with a finger. (d) Extracted  $C_{XY}$  variations from the Q3D Extractor model versus the contact thickness. The simulation proposes that a thickness of contact below 80  $\mu\text{m}$  leads to extreme electrical noise, disturbing the electrical reliability of the Cap-TSP.

### C. Prototype Assembly and Evaluation

Fig. 7 shows the measured  $C_{XY}$  sensing capacitance variations (Hawkeye program, ATMEL) versus the reference capacitance ( $C_{\text{ref}}$ ) in order to verify the electrical signal stability of the Cap-TS with/without the OLED display. The  $X$ – $Y$  coordinates are expressed as the touch location in a 4-in touch screen; the  $z$ -axis is the change in the sensing capacitance to reference ratio ( $C_{\text{sen}}/C_{\text{ref}}$ ) when sampling the sensing capacitance of the TSP. For the original electrical signal from TSP, as shown in

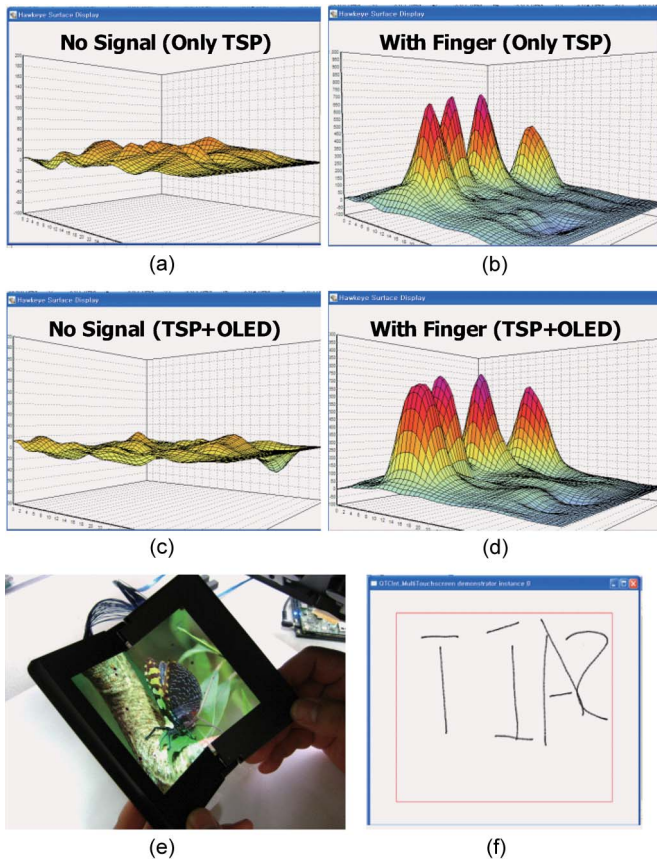


Fig. 7. Measured touch signal with respect to the readout frame. (a) Negligible noise signal without touch signal in a touch sensor. (b) Four-point multitouch shows a signal-to-noise ratio of  $\sim 500$ . The measured touch signal used the Cap-TSP integrated with the OLED. The lack of variation in the noise and touch signals demonstrates that a  $100\text{-}\mu\text{m}$ -thick OCA film, which was introduced by the Q3D Extractor, can isolate the electrical signal noise between the Cap-TSP and OLED panel. (c) Fabricated foldable/seamless OLED display. (f) Detected signal obtained from the experimental touch screen using a finger.

Fig. 7(a), the sensing capacitance with a finger is typically two orders of magnitude higher than the reference capacitance. A sensing variation will work in the two-order range, but smaller and larger signals can lead to the electrical malfunction of the TSP system. Based on the theoretical simulation, the low-dielectric OCA film thicker than  $80\text{ }\mu\text{m}$  allows the TSP to operate malfunction free without the losses from the fringe electrical field to the OLED cathode. Fig. 7(c) and (d) demonstrates the stability of the TSPs integrated onto the OLEDs with a  $100\text{-}\mu\text{m}$ -thick OCA film. Only negligible variations in the electrical signal were observed in both the TSP and the TSP with OLED panels. Fig. 7(b) and (d) illustrates multiple touches, where our capacitive touch sensor is interpreted as a signal using a mutual capacitive array so that the capacitive coupling at each point in the matrix can be sensed independently (Table I).

Fig. 7(e) shows a foldable/seamless 5.4-in OLED display embedded with two Cap-TSPs. We previously reported the fabrication of a prototype foldable/seamless OLED display. The ultrathin OLED platform, which was fabricated by advanced thin-film encapsulation and a capacitive touch sensor comprising a coplanar ITO layer, can allow for the removal of the visible crease of the folding structure and to be manufactured

TABLE I  
PROTOTYPE OF FOLDABLE/SEAMLESS OLED DISPLAY

Display size	7.0 mm X 172.8 mm (5.4" diagonal)
Touch Sensor	Cap-TSP, Atmel
Backplane substrate	$550\text{ }\mu\text{m}$ thick Ashahi glass
Cover glass	$550\text{ }\mu\text{m}$ thick Gorilla glass
Resolution	WVGA (800 X 480)
TFT structure	LTPS (Top Emission)
Encapsulation method	Thin film encapsulation

as an ultrathin display platform, compared with the reported current display. The physical thickness of our OLED display platform, excluding the two supporting glass layers (Ashahi, Gorilla glass), is approximately designed to have a thickness of  $130\text{ }\mu\text{m}$ . Furthermore, a possible application of the present ultrathin OLED platform can be extended to a flexible OLED display by replacing the two glass substrates with two supporting plastic layers applied in a proof-of-concept neutral plane. The development of an optimized plastic substrate and the low-temperature process used for fabricating a flexible OLED display and Cap-TSP represents some new directions for future displays.

#### IV. CONCLUSION

Without a doubt, AMOLED displays with touch screen capability will emerge as a future intuitive user interface. This paper has presented the first demonstration of highly sensitive capacitive touch sensors integrated into an ultrathin-film-encapsulated AMOLED display. The malfunction-free capacitive touch sensor has been fabricated as a coplanar/single-TIO layer and has a high 90% transparency. An OCA film with a low dielectric constant ( $\epsilon_r = 1.4$ ) has also been used to isolate the electrical signal noise between the touch sensor and OLED. In order to provide a quantitative analysis regarding the sensing mechanism, theoretical calculations on capacitor sensing between the human and touch electrodes, together with electromagnetic simulations regarding the electrical signal interference, have also been presented in this paper. All the processes used to fabricate the touch sensor have been developed to operate at low temperatures below  $200\text{ }^\circ\text{C}$ . The prototype capacitive touch sensor OLED platform exhibits a 1.2-mm thickness, which is the lowest thickness found for commercial OLED platforms.

#### ACKNOWLEDGMENT

The authors would like to thank ATMEL Inc., for supplying the driving IC chip and G. Kim of ATMEL Inc., for supporting and setting up a mutual capacitive touch screen panel.

#### REFERENCES

- [1] D.-U. Jin, T.-W. Kim, H.-W. Koo, D. Stryakhilev, H.-S. Kim, S.-J. Seo, M.-J. Kim, H.-K. Min, H.-K. Chung, and S.-S. Kim, "Highly robust flexible AMOLED display on plastic substrate with new structure," *Soc. Inf. Display (SID) Symp. Dig.*, vol. 47, no. 1, pp. 703–705, May 2010.
- [2] S. An, J. Lee, Y. Kim, T. Kim, D. Jin, H. Min, H. Chung, and S. S. Kim, "2.8-inch WQVGA flexible AMOLED using high performance

- low temperature polysilicon TFT on plastic substrate,” *Soc. Inf. Display (SID) Symp. Dig.*, vol. 47, no. 2, pp. 706–709, May 2010.
- [3] S. Kim, H.-J. Kwon, S. Lee, H. Shim, Y. Chun, W. Choi, J. Kwack, D. Han, M. Song, S. Kim, S. Mohammadi, S. Kee, and S. Y. Lee, “Low-power flexible organic light-emitting diode display device,” *Adv. Mater.* [Online]. Available: <http://onlinelibrary.wiley.com/doi/10.1002/adma.201101066/full>
- [4] H. Shim, I. Kee, S. Kim, Y. Chun, H. Kwon, Y. Jin, S. Lee, D. Han, J. Kwack, D. Kang, H. Seo, M. Song, M. Lee, and S. Kim, “A new seamless foldable OLED display composed of multi display panels,” *Soc. Inf. Display (SID) Symp. Dig.*, vol. 41, no. 1, pp. 257–260, May 2010.
- [5] H. Kwon, H. Shim, S. Kim, W. Choi, Y. Chun, I. Kee, and S. Lee, “Mechanically and optically reliable folding structure with a hyperelastic material for seamless foldable displays,” *Appl. Phys. Lett.*, vol. 98, no. 15, pp. 15 194–15 196, Apr. 2011.
- [6] M. Noda, N. Kobayashi, M. Katsuhara, A. Yumoto, S. Ushikura, R. Yasuda, N. Hirai, G. Yukawa, I. Yagi, K. Nomoto, and T. Urabe, “A rollable AM-OLED display driven by OTFTs,” *Soc. Inf. Display (SID) Symp. Dig.*, vol. 41, no. 1, pp. 710–713, May 2010.
- [7] Z. Suo, Z. E. Ma, H. Gleskova, and S. Wanger, “Mechanics of rollable and foldable film-on-foil electronics,” *Appl. Phys. Lett.*, vol. 74, no. 8, pp. 11 177–11 179, Feb. 1999.
- [8] S. Park, J. Ahn, X. Feng, S. Wang, Y. Huang, and J. A. Rogers, “Theoretical and experimental studies of bending of inorganic electronics materials on plastic substrates,” *Adv. Funct. Mater.*, vol. 18, no. 18, pp. 2673–2684, Sep. 2008.
- [9] W. P. Eaton and J. H. Smith, “Micromachined pressure sensors: Review and recent developments,” *Smart Mater. Struct.*, vol. 6, no. 5, pp. 530–539, May 1997.
- [10] S. P. Hotelling, J. A. Strickon, and B. Q. Huppi, “Multipoint touch screen,” U.S. Patent 10 840 862, May 11, 2006.
- [11] S. P. Hotelling and B. R. Land, “Double-sided touch-sensitive panel with shield and drive combined layer,” U.S. Patent 10 840 862, May 11, 2006.
- [12] S. P. Hotelling, C. H. Krah, and B. Q. Huppi, “Multipoint touch surface controller,” U.S. Patent 11 381 313, Nov. 8, 2007.
- [13] R. Adler and P. J. Desmares, “An economical touch panel using SAW absorption,” *IEEE Trans. Ultrason., Ferroelectr., Freq. Control*, vol. UFFC-34, no. 2, pp. 195–201, Mar. 1987.
- [14] S. H. Bae, B. C. Yu, S. Lee, H. U. Jang, J. Choi, M. Sohn, I. Ahn, I. Kang, and I. Chung, “Integrating multi-touch function with a large-sized LCD,” *Soc. Inf. Display (SID) Symp. Dig.*, vol. 39, no. 1, pp. 178–181, May 2008.
- [15] S. Pietri, A. Olmos, M. Berens, A. V. Boas, and M. Goes, “A fully integrated touch screen controller base on 12b 825 kS/s SAR ADC,” in *Proc. EAMTA*, May 2008, vol. 39, no. 1, pp. 178–181.
- [16] W. Buller and B. Wilson, “Measurement and modeling mutual capacitance of electrical wiring and humans,” *IEEE Trans. Instrum. Meas.*, vol. 55, no. 5, pp. 1519–1522, Oct. 2006.
- [17] *Introduction to Capacitive Sensing*, Microchip Technol. Inc., Chandler, AZ, 2007. [Online]. Available: <http://ww1.microchip.com/downloads/en/AppNotes/011101a.pdf>
- [18] *Capacitive Touch Sensors*, Fujitsu Microelectron., Langen, Germany, 2010. [Online]. Available: <http://www.fujitsu.com/downloads/MICRO/fme/articles/fujitsu-whitepaper-capacitive-touch-sensors.pdf>
- [19] H. Morimura, S. Shigematsu, and K. Machida, “A novel sensor cell architecture and sensing circuit scheme for capacitive fingerprint sensors,” *IEEE J. Solid-State Circuits*, vol. 35, no. 5, pp. 724–731, May 2000.
- [20] J. Carey, “Dealing with capacitance sensor algorithm in multitouch sensing,” *EETimes*, Sep. 2009. [Online]. Available: [http://www.eetasia.com/ART\\_8800584055\\_480500\\_TA\\_9dc57e79.htm](http://www.eetasia.com/ART_8800584055_480500_TA_9dc57e79.htm)

Authors’ photographs and biographies not available at the time of publication.